Author's personal copy

Available online at www.sciencedirect.com

ScienceDirect

Advances in Space Research 53 (2014) 1219–1228

ADVANCES IN SPACE RESEARCH (a COSPAR publication)

www.elsevier.com/locate/asr

The classical Laplace plane as a stable disposal orbit for geostationary satellites

Aaron J. Rosengren *, Daniel J. Scheeres, Jay W. McMahon

Department of Aerospace Engineering Sciences, University of Colorado at Boulder, Boulder, CO 80309, USA

Received 6 November 2013; received in revised form 28 January 2014; accepted 30 January 2014
Available online 6 February 2014

Abstract

The classical Laplace plane is a frozen orbit, or equilibrium solution for the averaged dynamics arising from Earth oblateness and lunisolar gravitational perturbations. The pole of the orbital plane of uncontrolled GEO satellites regress around the pole of the Laplace plane at nearly constant inclination and rate. In accordance with Friesen et al. (1993), we show how this stable plane can be used as a robust long-term disposal orbit. The current graveyard regions for end-of-life retirement of GEO payloads, which is several hundred kilometers above GEO depending on the spacecraft characteristics, cannot contain the newly discovered high area-to-mass ratio debris population. Such objects are highly susceptible to the effects of solar radiation pressure exhibiting dramatic variations in eccentricity and inclination over short periods of time. The Laplace plane graveyard, on the contrary, would trap this debris and would not allow these objects to rain down through GEO. Since placing a satellite in this inclined orbit can be expensive, we discuss some alternative disposal schemes that have acceptable cost-to-benefit ratios.
© 2014 COSPAR. Published by Elsevier Ltd. All rights reserved.

Keywords: Geosynchronous orbit; High area-to-mass ratio objects; Space debris; Disposal orbits; Celestial mechanics; Dynamical evolution and stability

1. Introduction

Nearly a half century has elapsed since satellites were first launched into the geostationary (equatorial, circular-synchronous) orbit—the altitude of 35,786 km where satellites appear to remain fixed over a single point on the equator throughout the day, providing a unique vantage point for communication, meteorology, science, and military applications (Zee, 1989; Johnson, 2012). The geostationary ring is the least forgiving region to space debris because there is no natural cleansing mechanism to limit the lifetimes of the debris at this altitude. Only objects in low-altitude orbits will return to Earth without human intervention through the influence of atmospheric drag, which steadily reduces their orbital energy until they re-enter or burn up within the atmosphere. In some preferential low Earth orbit (LEO) regions, where the population is above a critical spatial density, random collisions are predicted to produce new debris at a rate that is greater than the removal rate due to orbital decay (i.e., the Kessler syndrome; see, for instance, Kessler and Cour-Palais, 1978; Liou and Johnson, 2006). In GEO, the relative velocities are much lower (less than 1 km/s), meaning that the the damage done by impact and the amount of detritus generated in a collision is not as severe. However, because debris would contaminate this unique and valuable resource practically forever, placing satellites in super-synchronous disposal orbits at the ends of their operational lifetimes has been recommended and practiced as one possible means of protecting this orbital environment (IADC, 2007; ITU, 2010). These satellites are also passivated to

* Corresponding author. Tel.: + 1 303 492 7826.
E-mail addresses: aaron.rosengren@colorado.edu (A.J. Rosengren), scheeres@colorado.edu (D.J. Scheeres), mcmahojw@colorado.edu (J.W. McMahon).

http://dx.doi.org/10.1016/j.asr.2014.01.034
0273-1177/© 2014 COSPAR. Published by Elsevier Ltd. All rights reserved.

Author's personal copy

reduce the probability of future explosions by removing any on-board stored energy, such as residual fuel or pressurants and charged batteries.

The high area-to-mass ratio (HAMR) debris population in GEO space, discovered through optical observations by Schildknecht et al. (2004), demonstrates that energetic breakups and collisions are not the only source of concern (Schildknecht, 2007). This hitherto unknown class of body—having area-to-mass ratios hundreds or thousands of times greater than that of a typical satellite and thus strongly perturbed by solar radiation pressure (SRP)—has been linked to aging satellites in the storage orbits (Liou and Weaver, 2005). Such objects can be generated in a variety of ways: material deterioration, surface degradation, collisions, and explosions, to name just a few. The low energy release of HAMR objects from aging satellites abandoned in disposal orbits is not directly addressed in the international policies that established the graveyard (IADC, 2007; Johnson, 2012). The current disposal region, which is several hundred kilometers above GEO, is not well suited as a graveyard for two important reasons: it does not mitigate the possibility of collisions between the uncontrolled objects residing in this region,[1] and it cannot contain the HAMR population.

In geostationary orbit, station–keeping maneuvers are required to constantly maintain the orderly arrangements of operational satellites. The orbital dynamics of uncontrolled geostationary satellites is governed by the oblateness (equatorial bulge) of the Earth and third-body gravitational interactions induced by the Sun and the Moon (lunisolar perturbations). By itself, Earth's oblateness causes the pole of the orbital plane to precess around Earth's rotation pole. Lunisolar perturbations, if acting alone, will have a similar effect, but the precession will now take place about the poles of the orbital planes of the Moon and the Sun, respectively. The motion of the orbit pole of the satellite is a combination of simultaneous precession about these three different axes, one of which, the pole of the Moon's orbit, regresses around the pole of the ecliptic with a period of 18.61 years. The classical Laplace plane is the mean reference plane about whose axis the satellite's orbit precesses (Allan and Cook, 1964; Tremaine et al., 2009).

A circular orbit in the classical Laplace plane experiences no secular precession; thus, the Laplace plane is simply a frozen orbit, or equilibrium solution for the averaged dynamics arising from the quadrupole potential of the gravitational perturbations (Tremaine et al., 2009). Under the assumption that the lunar orbit lies in the ecliptic, Allan and Cook found an approximate Laplace plane at GEO, which lies between the plane of the Earth's equator and that of the ecliptic and passes through their intersection (the vernal equinox), and which has an inclination of about 7.2° with respect to the equator (Allan and Cook, 1964). The geostationary satellites, following cessation of active station–keeping, precess at a constant inclination about the pole of the Laplace plane with a period of nearly 53 years (Friesen et al., 1992; Friesen et al., 1993; Schildknecht, 2007). Sufficient time has now passed for the orbits of the earliest uncontrolled satellites to complete their long-period motion, as indicated by Schildknecht, 2007.

In the early 1990s, when the problems of overcrowding of geostationary orbit with operational and defunct satellites began to emerge, Friesen et al. (1992) suggested the use of the classical Laplace plane for satellite applications and as an orbital debris management strategy for GEO orbit (Friesen et al., 1992; Friesen et al., 1993). The orbit plane of a geosynchronous satellite with such an orientation, notes Otis Graf, would be fixed in space (Graf et al., 1975). The significance of the Laplace plane for use as a GEO disposal orbit is that the orbits of satellites placed in this stable equilibrium will be fixed on average, and that any orbit at small inclination to it regresses around this plane at nearly constant inclination and rate (Allan and Cook, 1964). This stable graveyard can be specified for a range of semi-major axes above (or below) GEO, and satellites located in this region will have drastically reduced relative encounter velocities, compared to the conventional graveyard orbits (Friesen et al., 1993). Thus, if collisions were to occur between satellites in the stable graveyard, they would occur at very low velocities, thereby damping out the relative motion of these objects and keeping them in this stable plane.

The purpose of this paper is to investigate the robustness of the Laplace plane graveyard orbit to the recently discovered HAMR debris. We rigorously show how solar radiation pressure modifies the classical Laplace plane and discuss the implications of this result for the HAMR objects. We also discuss the economic viability of the Laplace graveyard and propose an alternative disposal scheme, which takes advantage of the dynamics and stability of GEO orbits.

2. Frozen orbits in the Earth–Moon–Sun system

2.1. The classical Laplace plane

The orbital geometry can be described naturally and succinctly in terms of the angular momentum and eccentricity vectors (i.e., the Milankovitch elements; see Milankovitch, 1941; Rosengren and Scheeres, 2014):

$$\boldsymbol{H} = \tilde{\boldsymbol{r}} \cdot \boldsymbol{v}, \tag{1}$$

[1] There is circumstantial evidence that collisions have occurred in the super-synchronous disposal regime. For instance, the decommissioned GOES-10 NOAA spacecraft (International Designator 1997-019A, U.S. Satellite Number 24786) experienced a distinct change in orbital period on 5 September 2011, abruptly falling to a slightly lower orbit in the graveyard region above GEO. As the derelict GOES-10 spacecraft had been completely passivated, the cause of this anomalous orbital perturbation might have been from an impact with an unknown object (NASA, 2012).

Author's personal copy

$$\boldsymbol{e} = \frac{1}{\mu}\widetilde{\boldsymbol{v}} \cdot \boldsymbol{H} - \frac{\boldsymbol{r}}{|\boldsymbol{r}|}, \tag{2}$$

where $\boldsymbol{r}$ and $\boldsymbol{v}$ are the position and velocity vectors, and the notation $\widetilde{\boldsymbol{a}}$ denotes the cross-product dyadic, defined such that $\widetilde{\boldsymbol{a}} \cdot \boldsymbol{b} = \boldsymbol{a} \cdot \widetilde{\boldsymbol{b}} = \boldsymbol{a} \times \boldsymbol{b}$ for any vectors $\boldsymbol{a}, \boldsymbol{b}$ in $\boldsymbol{R}^3$. These vectors have a clear geometrical significance: $\boldsymbol{H}$ points perpendicular to the instantaneous orbit plane and has magnitude (for elliptical orbits) $H = \sqrt{\mu a(1-e^2)}$; $\boldsymbol{e}$ defines the orientation of the major axis in the orbital plane, pointing towards the instantaneous periapsis of the orbit, and its magnitude is the eccentricity. Recall the basic definition of these vectors in terms of the Keplerian orbital elements relative to an inertial frame:

$$\boldsymbol{H} = H\hat{\boldsymbol{h}} = H(\sin i \sin\Omega\hat{\boldsymbol{x}} - \sin i \cos\Omega\hat{\boldsymbol{y}} + \cos i\,\hat{\boldsymbol{z}}), \tag{3}$$

$$\begin{aligned}\boldsymbol{e} = e\hat{\boldsymbol{e}} = e[&(\cos\omega\cos\Omega - \cos i \sin\omega\sin\Omega)\hat{\boldsymbol{x}} \\ &+ (\cos\omega\sin\Omega + \cos i \sin\omega\cos\Omega)\hat{\boldsymbol{y}} + \sin i \sin\omega\hat{\boldsymbol{z}}],\end{aligned} \tag{4}$$

where μ is the gravitational parameter, a the semi-major axis, e the eccentricity, i the inclination, Ω the right ascension of the ascending node, and ω the argument of periapsis. As the relationship between the classical orbit elements and $\boldsymbol{H}$ and $\boldsymbol{e}$ are complex, we find it simpler to rely on the geometric definition of these vectors.

In secular dynamics, the semi-major axis is fixed and the problem can be reduced to understanding the evolution of the scaled angular momentum vector $\boldsymbol{h} = \boldsymbol{H}/\sqrt{\mu a}$ and the eccentricity vector $\boldsymbol{e}$. Considering only gravitational perturbations and assuming that the lunar orbit lies in the ecliptic, the secular equations of motion arising from Earth oblateness and lunisolar perturbations can be stated as (Allan and Cook, 1964; Tremaine et al., 2009; Rosengren et al., 2013a)

$$\dot{\boldsymbol{h}} = -\frac{\omega_2}{h^5}(\hat{\boldsymbol{p}}\cdot\boldsymbol{h})\widetilde{\hat{\boldsymbol{p}}}\cdot\boldsymbol{h} - (\omega_m+\omega_s)\hat{\boldsymbol{H}}_s\cdot(5\boldsymbol{e}\boldsymbol{e} - \boldsymbol{h}\boldsymbol{h})\cdot\widetilde{\hat{\boldsymbol{H}}}_s, \tag{5a}$$

$$\begin{aligned}\dot{\boldsymbol{e}} = &-\frac{\omega_2}{2h^5}\left\{\left[1 - \frac{5}{h^2}(\hat{\boldsymbol{p}}\cdot\boldsymbol{h})^2\right]\widetilde{\boldsymbol{h}} + 2(\hat{\boldsymbol{p}}\cdot\boldsymbol{h})\widetilde{\hat{\boldsymbol{p}}}\right\}\cdot\boldsymbol{e} \\ &-(\omega_m+\omega_s)\left[\hat{\boldsymbol{H}}_s\cdot(5\boldsymbol{e}\boldsymbol{h} - \boldsymbol{h}\boldsymbol{e})\cdot\widetilde{\hat{\boldsymbol{H}}}_s - 2\widetilde{\boldsymbol{h}}\cdot\boldsymbol{e}\right],\end{aligned} \tag{5b}$$

in which $\hat{\boldsymbol{p}}$ is a unit vector aligned with the maximum axis of inertia of the Earth (i.e., Earth's rotation pole), $\hat{\boldsymbol{H}}_s$ is a unit vector aligned with the angular momentum vector of the Sun's orbit (i.e., Earth's orbit pole), and

$$\omega_2 = \frac{3nJ_2R^2}{2a^2}, \quad \omega_p = \frac{3\mu_p}{4na_p^3(1-e_p^2)^{3/2}}, \tag{6}$$

where $n = \sqrt{\mu/a^3}$ is the satellite's mean motion, J_2 is the oblateness gravity field coefficient, R is the mean equatorial radius of the Earth, and μ_p, a_p, and e_p are the gravitational parameter, semi-major axis, and eccentricity, respectively, of the perturbing body (Moon or Sun). We assume that the Earth's spin axis $\hat{\boldsymbol{p}}$ is fixed in inertial space, thereby neglecting the tidal torques on the Earth's equatorial bulge as this precession period is much longer than the precession period of the satellite orbit (Milankovitch, 1941; Boué and Laskar, 2006)

Tremaine et al. (2009) defines the Laplace equilibria to be stationary solutions of Eq. (5), or orbits where the average angular momentum and eccentricity vectors remain constant. There are five types of equilibria for the system, each classified by the orientation of the vectors $\boldsymbol{h}$ and $\boldsymbol{e}$. For an initially circular orbit, $\dot{\boldsymbol{e}}$ is identically zero and the orbit will remain circular throughout. There are two kinds of equilibria in this case: the polar Laplace equilibrium and the classical Laplace plane. See Tremaine et al. (2009) for details on the stability of the polar Laplace equilibrium; its application to Earth orbiters is given in Kudielka (1994) and Ulivieri et al. (2013). We consider only the classical Laplace plane equilibrium which is defined as the circular Laplace equilibria ($\boldsymbol{e} = \boldsymbol{0}$) for which $\boldsymbol{h}$ lies in the principal plane specified by the vectors $\hat{\boldsymbol{p}}$ and $\hat{\boldsymbol{H}}_s$. It may be parameterized by an azimuthal angle φ, as shown in Fig. 1, where ϵ is the obliquity of the ecliptic (*i.e.*, the angle between the Earth's equatorial plane and orbit). The frozen orbit condition becomes (Allan and Cook, 1964; Rosengren et al., 2013a; Tremaine et al., 2009)

$$\omega_2 \sin 2\varphi + (\omega_m + \omega_s)\sin 2(\varphi - \epsilon) = 0 \quad \text{or}$$

$$\tan 2\varphi = \frac{\sin 2\epsilon}{\cos 2\epsilon + (r_L/a)^5}, \tag{7}$$

where r_L is the Laplace radius defined by

$$r_L^5 = a^5\frac{\omega_2}{\omega_m + \omega_s}. \tag{8}$$

Eq. (7) has four solutions for φ in a 2π interval. The classical Laplace surface is the prograde circular orbit that has the properties $\varphi \to 0$ as $a \to 0$ and $\varphi \to \epsilon$ as $a \to \infty$, so that it coincides with the Earth's equator at small geocentric distances and with its orbital plane at large distances (Tremaine et al., 2009). The Laplace radius is the critical distance at which the Laplace plane lies halfway between the equatorial and ecliptic planes: it is thus the geocentric

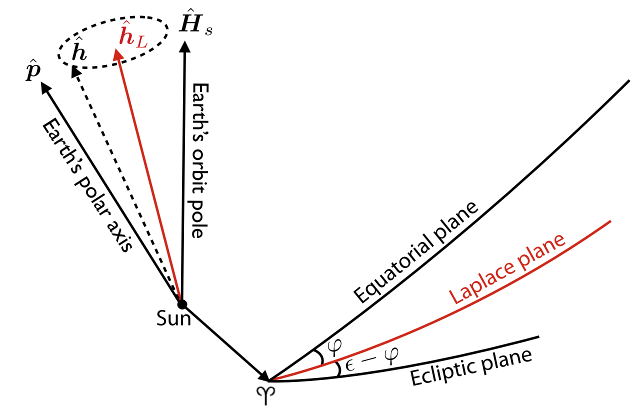

Fig. 1. Geometry of the Laplace plane equilibrium. The pole $\hat{\boldsymbol{h}}$ of any orbit at small inclination to the pole of the Laplace plane will regress about $\hat{\boldsymbol{h}}_L$ at constant inclination and rate.

Author's personal copy

distance where the effects of oblateness and lunisolar forces are equal. Note that for Earth-orbital dynamics, this equilibrium is stable to both changes in the orbit plane orientation and eccentricity (Tremaine et al., 2009).

Shown in Fig. 2 is the long-term evolution of the inclination and ascending node, in the Earth equatorial frame, of initially geostationary satellites. These (uncontrolled) satellites precess at a nearly constant inclination about the pole of the Laplace plane with a period of about 53 years. The orbital planes of these objects evolve in a predictable way; that is, their inclinations and ascending nodes are strongly correlated (see Fig. 2a). In fact, the former Soviet Union designed their geostationary satellite constellation to take advantage of this systematic structure: by selecting the initial inclination and ascending node such that the perturbations will naturally reduce the inclination to zero before increasing again, the satellite's inclination is kept below a few degrees over its lifetime without the need of expensive north–south station–keeping (Johnson, 1982; Johnson, 2012).

2.2. The modified Laplace plane

Solar radiation pressure is the largest non-gravitational perturbative force to affect the motion of HAMR objects in high-Earth orbits, causing extreme changes in their orbital parameters over short time periods. Allan and Cook (1967), during their investigation of the zodiacal light, showed that solar radiation pressure modifies the classical Laplace plane equilibrium for small dust grains in high Earth orbit. They found an approximate solution to the modified Laplace plane and noted that the orbital plane of a given dust particle, for a given semi-major axis, will regress around this plane. In particular, they found that the angular momentum vector would have a secular precession period in years of $2/e_m^2$, where e_m is the maximum eccentricity attained during the year (provided that $e_m^2 \ll 1$). Through comparisons with a high-fidelity orbit integrator, Friesen et al. (1992) showed that Allan and Cook's predictions are limited to particles that are only weakly perturbed by solar radiation pressure; that is, particles which have low values of effective area-to-mass ratio. There has hitherto been no analytical theory capable of giving an accurate prediction of the modified Laplace plane equilibrium.

From a previously derived solution for the secular motion of an orbiter about a small body (asteroid or comet) in a solar radiation pressure dominated environment (Richter and Keller, 1995; Scheeres, 2012), we have found that SRP acting alone will have a precisely similar secular effect on initially circular orbits as solar gravitational perturbations, causing the orbit to precess around the pole of the ecliptic in accordance with the prediction of Allan and Cook (1967), but with the rate of rotation being $(1 - \cos\Lambda)/\cos\Lambda$, where Λ is the SRP perturbation angle defined as (Mignard and Hénon, 1984).

$$\tan\Lambda = \frac{3\beta}{2V_{lc}H_s}, \tag{9}$$

in which $\beta = (1+\rho)(A/m)P_\Phi$, ρ is the total reflectance or albedo of the body, A/m is the appropriate cross-sectional area-to-mass ratio in m^2/kg, P_Φ is the solar radiation constant ($\sim 1\times10^8$ kg km^3/s^2/m^2), V_{lc} is the local circular speed of the object about the Earth, and H_s is the specific angular momentum of the Earth about the Sun. Note that as the perturbation becomes strong, $\Lambda \to \pi/2$; and as it becomes weak $\Lambda \to 0$.

Including the secular effect of SRP into Eq. (5), we can find an approximate mean pole around which the orbit precesses. The condition for the modified equilibrium becomes

$$\omega_2(\hat{\boldsymbol{p}}\cdot\hat{\boldsymbol{h}})\tilde{\hat{\boldsymbol{p}}}\cdot\hat{\boldsymbol{h}}+(\omega_m+\omega_s)(\hat{\boldsymbol{H}}_s\cdot\hat{\boldsymbol{h}})\widetilde{\hat{\boldsymbol{H}}}_s\cdot\hat{\boldsymbol{h}}+\omega_{srp}\widetilde{\hat{\boldsymbol{H}}}_s\cdot\hat{\boldsymbol{h}}=\boldsymbol{0} \quad \text{or} \tag{10}$$

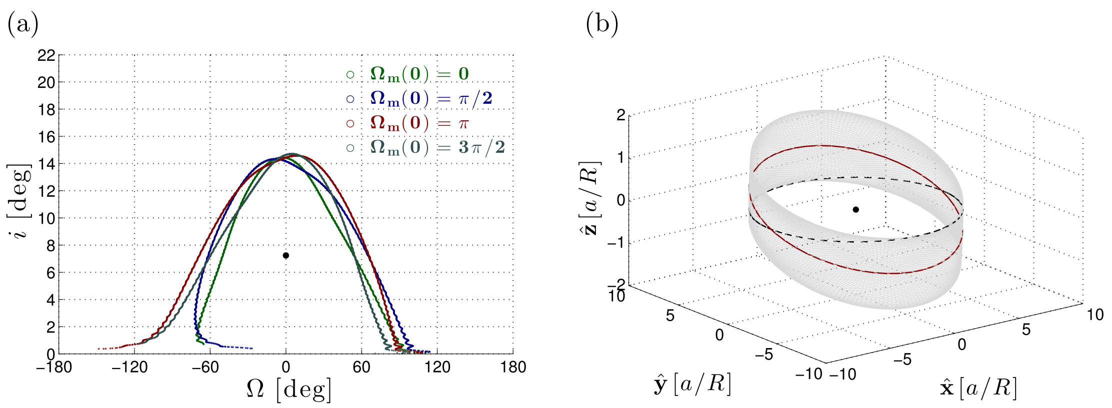

Fig. 2. Long-term motion, in the Earth-equatorial frame, of the orbital plane of initially geostationary satellites. A numerical integration was performed over 53 years of an averaged model developed in Rosengren and Scheeres (2013) for four different initial positions of the lunar orbit, i.e., four different launch dates as follows: July 1964 ($\Omega_m(0) = \pi/2$), March 1969 ($\Omega_m(0) = 0$), November 1973 ($\Omega_m(0) = 3\pi/2$), July 1978 ($\Omega_m(0) = \pi$). (a) Scatter plot of the time-series, over 53 years, of inclination and ascending node as predicted by an averaged model. The classical Laplace plane has $i = 7.2°$ and $\Omega = 0°$ as indicated by the black dot. (b) Three-dimensional picture of the evolution of one of the satellites. The Earth is at the center, the initial geostationary orbit is indicated by the black orbit, and the classical Laplace plane is shown in red. The Laplace plane is the plane of symmetry for the evolution.

Author's personal copy

$$\omega_2 \sin 2\varphi + (\omega_m + \omega_s) \sin 2(\varphi - \epsilon) + 2\omega_{srp} \sin(\varphi - \epsilon) = 0, \tag{11}$$

where

$$\omega_{srp} = \frac{2\pi(1 - \cos\Lambda)}{T_s \cos\Lambda}, \tag{12}$$

and T_s is the Earth's orbital period in seconds.

The orientation of the modified Laplace surface between the degenerate states (equatorial and ecliptic) is given as a function of a/R in Fig. 3. Solar radiation pressure modifies the classical Laplace plane, increasing its inclination relative to the equator with increasing Λ; each HAMR objects has its own modified Laplace plane for a given semi-major axis and effective area-to-mass ratio (or corresponding modified Laplace surface).

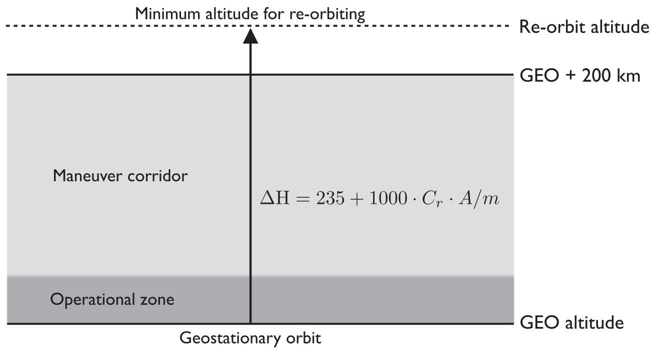

Fig. 4. The current, internationally established, disposal scheme for end-of-life retirement of GEO payloads. The accepted re-orbiting altitude is specified by ΔH, which accounts for the geostationary protected region and an allowance for perigee oscillation due to gravitational and non-gravitational perturbations (Adapted from ITU, 2010).

3. The Laplace plane graveyard orbit

The current disposal orbit scheme, established by the Inter-Agency Space Debris Coordination Committee and supported by the International Telecommunication Union, is to boost retired satellites into super-synchronous orbits several months before station–keeping fuel is expected to be exhausted (IADC, 2007; ITU, 2010). The minimum altitude threshold for re-orbiting incorporates the geostationary protected region (i.e., the operational station–keeping zone and maneuver corridor) as well as an allowance for gravitational and non-gravitational perturbations, as shown in Fig. 4. The stability of the super-synchronous disposal orbits and their potential to reduce collision hazards have been investigated extensively in the literature (Hechler and Van der Ha, 1981; Johnson, 2012); however, these studies have focused on long-term simulations of intact satellites, which have very low area-to-mass ratios. We have found that this current disposal scheme for end-of-life retirement of GEO payloads is not well suited as a long-term graveyard because it does not mitigate the possibility of collisions between the uncontrolled objects residing in this region, nor does it reduce the severity of such collisions, and it cannot contain the high area-to-mass ratio debris population (Rosengren et al., 2013a,b; Schildknecht, 2007).

The long-term evolution of the orbital plane of HAMR objects, released from super-synchronous disposal orbits, is shown in Fig. 5(a). An increase in Λ results in a faster and wider clockwise precession of the orbit pole (Friesen et al., 1992; Anselmo and Pardini, 2010), with the secular precession period as a function of Λ given in Fig. 6. When HAMR objects return to zero inclination, which occurs much faster than the uncontrolled satellites, they may very rapidly cross the geostationary protected region due to their significant eccentricity oscillations (Fig. 7). More specifically, the probability of a particular debris object in the disposal orbit striking an active satellite in the GEO belt is largely dependent on the geometry of its orbital plane.

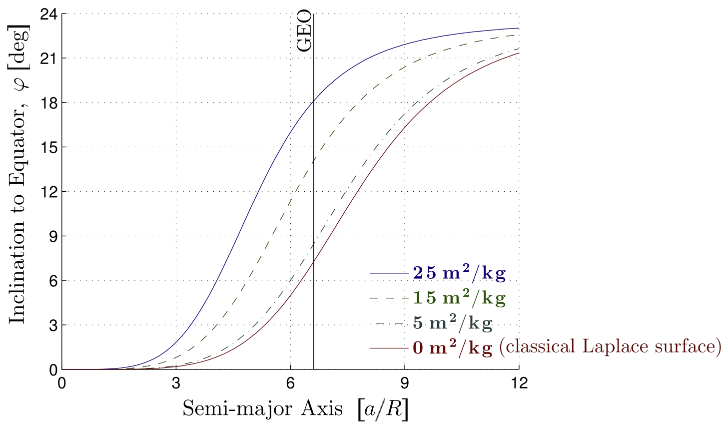

Fig. 3. Inclination of the Laplace plane equilibrium relative to the Earth's equator as a function of semi-major axis in Earth radii for a range of HAMR values. For an object near the Earth, the Laplace plane (both classical and modified) lies approximately in the Earth's equatorial plane, while for distant objects, it coincides with the ecliptic plane; all three planes sharing a common node (the vernal equinox). Between these two degenerate states, the Laplace plane at a given semi-major axis lies at some intermediate orientation, generating the warped Laplace surface. Note that an object with $A/m = 0\ \mathrm{m^2/kg}$ corresponds to the classical Laplace surface, shown as the bottom curve.

Author's personal copy

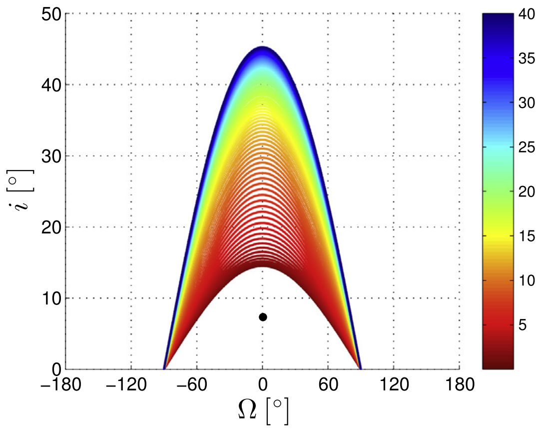

(a) Super-synchronous disposal orbit.

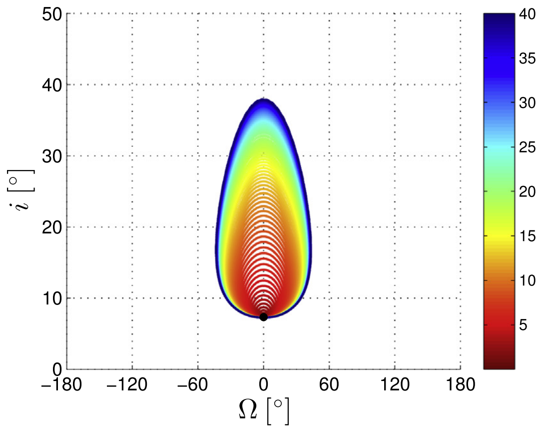

(b) Laplace plane disposal orbit.

Fig. 5. Qualitative evolution of the orbital planes of HAMR objects, released from geostationary orbit and from the classical Laplace plane, illustrating the nature of the problem. The colorbar indicates the value of Λ in degrees and the position of the classical Laplace plane is indicated by the black dot.

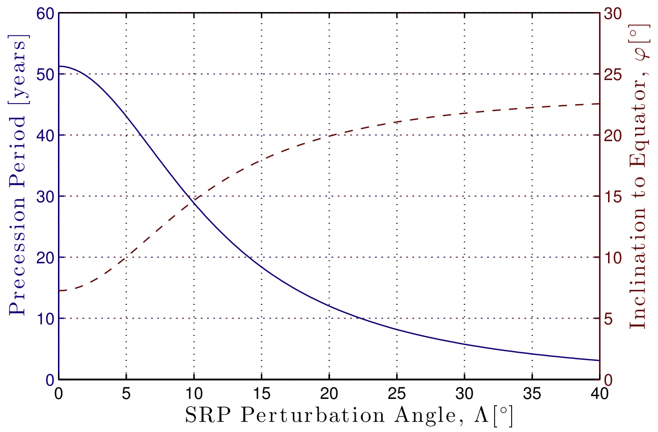

Fig. 6. Approximate secular precession period of the orbital pole as a function of Λ, and inclination of the modified Laplace plane equilibrium. The pole of the orbit precesses at constant rate and inclination around the approximate mean pole $\hat{\boldsymbol{h}}_L$ with a period $2\pi/\omega$, where $\omega\hat{\boldsymbol{h}}_L = \omega_2\hat{\boldsymbol{p}} + (\omega_m + \omega_s + \omega_{srp})\hat{\boldsymbol{H}}_s$. The modified Laplace plane is the plane of symmetry for the HAMR objects of Fig. 5.

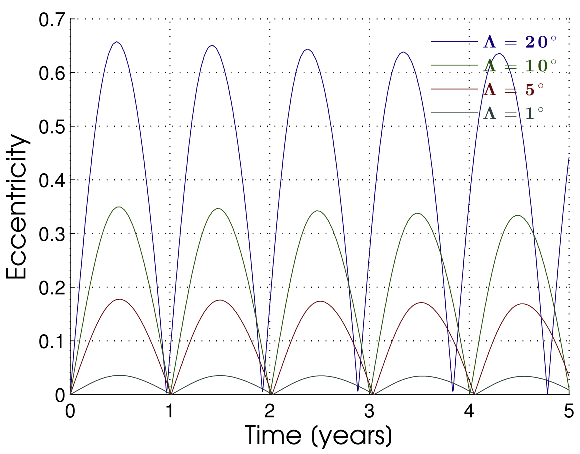

Fig. 7. Evolution of the orbit eccentricity for different values of the SRP perturbation angle. The eccentricity undergoes an approximately yearly oscillation with amplitude increasing with increasing Λ.

Evidently, for the objects to collide, their orbital paths must cross and they must arrive at the intersection at the same time. HAMR objects in eccentric orbits that are inclined to the equatorial plane will have a very small but non-zero probability of crossing the geostationary ring; however, HAMR objects that reside in the equatorial plane will have a high probability of impact because they will intersect this ring twice per orbit. For these reasons, we reconsider the possibility of using the stable Laplace plane equilibrium as a robust GEO graveyard, a notion originally put forward by Friesen et al. (1993), but which has not been fully appreciated in the scholarly world. Not only will satellites orbiting in this region have drastically reduced relative encounter velocities, thereby reducing the likelihood of a collisional cascade, but we have found that this region is robust to large SRP perturbations (Rosengren et al., 2013a,b). In particular, if satellites located in the classical Laplace plane graveyard orbit shed HAMR objects, they will be trapped in inclination and ascending node phase space, and will not likely cross the GEO protected region, as demonstrated in Fig. 5(b).

3.1. Nearness to reality

We now concern ourselves with the issue of realism. We called the Laplace plane a frozen orbit because it is an equilibrium for the averaged equations of motion. The method of averaging is based on the idea that the short-period terms discarded in averaging cause only small oscillations, which are superimposed on the drift described by the averaged system. The natural question arises as to whether the secular equilibrium will "unfreeze" when these short-term variations are included or when the averaging is pushed to higher order.

In Rosengren and Scheeres (2013), we developed and validated a singly-averaged, first-order model that accounts for planetary oblateness, lunisolar gravitational attraction,

Author's personal copy

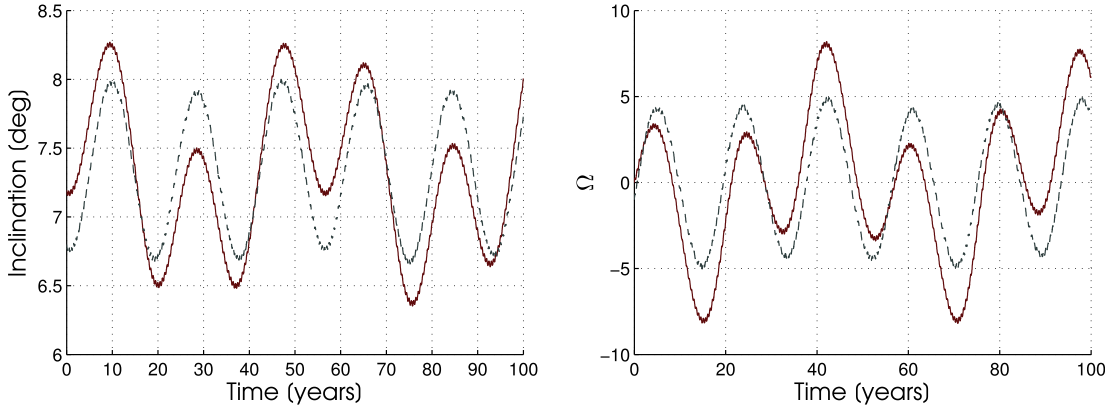

(a) Inclination evolution (b) Ascending node evolution

Fig. 8. Long-term evolution of the inclination and right ascension of the ascending node for a geosynchronous satellite released from the classical Laplace plane equilibrium, showing a comparison between our predicted result (red, solid curve) and the empirical result of Friesen et al. (1993) (gray, dashed curve). (For interpretation of the references to color in this figure legend, the reader is referred to the web version of this article.)

and solar radiation pressure. This model was shown to provide a very accurate description of the long-term behavior and can be used for accurate long-term predictions. Fig. 8 shows the evolution of the Laplace plane, as predicted by our averaged model. Note that the position vectors of both the Sun and the Moon were computed using the JPL ephemeris (DE421). The orbit planes of GEO satellites placed in such an orbit experience very little precession, remaining always within 1° of their initial orientation. As indicated by Friesen et al. (1993) and shown by the dashed curve, these excursions, which are caused by the regression of the lunar nodes, can be further reduced by choosing the initial orbit plane orientation to be in phase with the Moon's nodal precession.

Fig. 9(a) shows the time-series, over 100 years of inclination and right ascension of the ascending node in the Earth-equatorial frame, for several HAMR objects released from the super-synchronous disposal orbit. Fig. 9(b) shows the dynamical behavior of the orbital planes for the same objects released in the classical Laplace plane. The characteristics of the evolution, including the Saros secular resonance, are discussed in Rosengren and Scheeres (2013) and will be omitted here. The significant feature revealed by Fig. 9, and noted previously by Allan and Cook (1967), is that the modified Laplace plane at a given semi-major axis is a plane of symmetry for each object. Note that the qualitative behavior underlined by our approximate analysis is in excellent agreement with that shown here.

3.2. Robustness of Laplace graveyard to high-fidelity SRP models

The solution to the modified Laplace plane equilibrium and its implication to the high area-to-mass ratio debris are based on what is known in astrodynamical parlance as the

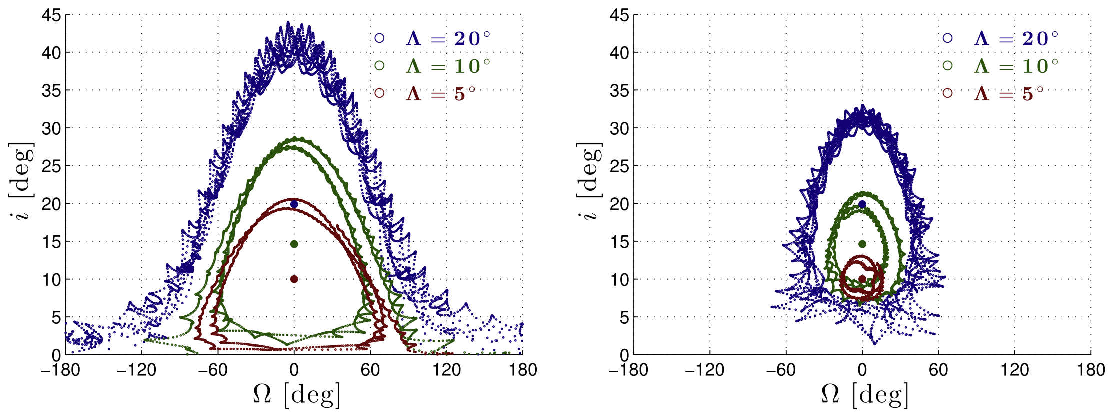

(a) Super-synchronous disposal orbit. (b) Laplace plane disposal orbit.

Fig. 9. Long-term motion, in the Earth-equatorial frame, of the orbital planes of HAMR objects as predicted by an accurate averaged model. The corresponding predicted equilibriums for each object are also shown. Note that the object with $\Lambda = 20^\circ$ represents an extreme case, being in near resonance with the lunar nodal regression (q.v., Rosengren and Scheeres, 2013). Objects outside of the resonance range ($\Lambda \leqslant 10^\circ.5$ and $\Lambda \geqslant 15^\circ.5$), if released from the Laplace graveyard, will not migrate significantly below their initial inclination.

Author's personal copy

cannonball model of solar radiation pressure, which treats the object as a sphere with constant optical properties. The net acceleration is assumed to be acting along the object-Sun line, which is taken to be parallel to the Earth-Sun line, and the total momentum transfer from the incident solar photons is modeled as insolation plus reflection. This attitude-independent model neglects any force component normal to the Earth-Sun line that results from an aspherical shape or nonuniformly reflecting surface. In some cases, depending on the rotational motion of the object, this non-radial component of the radiation pressure is negligible or will average out over time periods that are small compared to the orbital period. However, the validity of this frequently made assumption for debris, and HAMR objects in particular, may not be well established (Früh and Schildknecht, 2012; McMahon and Scheeres, 2013).

The direction of SRP acceleration is not, in general, directly away from the Sun, as indicated by the cannonball model. Rather, this direction depends on the shape of the object, its optical properties, and its orientation with respect to the Earth-Sun line. The total radiation pressure of the incident sunlight, assuming that the Sun acts as a point source, can be modeled to first order as

$$P(d_s) = \frac{P_\Phi}{d_s^2}, \tag{13}$$

where d_s is the distance between the Earth and the Sun. The net acceleration due to the solar photons can be written in the general form (Rosengren and Scheeres, 2014)

$$\boldsymbol{a}_{srp} = \frac{\beta'}{d_s^2}\hat{\boldsymbol{a}}, \tag{14}$$

in which $\hat{\boldsymbol{a}}$ is the net direction of the acceleration and

$$\beta' = \frac{P_\Phi|\sum_{i=1}^{N}\boldsymbol{F}_i|}{m}, \tag{15}$$

where $\boldsymbol{F}_i$ represents the solar radiation force acting on a unit area A and m is the total mass of the body. Accounting for the total momentum transfer of the solar photons striking and recoiling off the surface element of a general body, $\boldsymbol{F}_i$ can be specified as

$$\begin{aligned}\boldsymbol{F}_i = &-P(d_s)[\{\rho s(2\hat{\boldsymbol{n}}\hat{\boldsymbol{n}} - \boldsymbol{U}) + \boldsymbol{U}\} \cdot \hat{\boldsymbol{u}}\hat{\boldsymbol{u}} \cdot \hat{\boldsymbol{n}} + \{B(1-s)\rho \\ &+ (1-\rho)B\}\hat{\boldsymbol{n}}\hat{\boldsymbol{n}} \cdot \hat{\boldsymbol{u}}]H(\hat{\boldsymbol{u}})A\end{aligned} \tag{16}$$

where s is the fraction of specularly reflected light, $\hat{\boldsymbol{n}}$ is the unit normal to the surface, $\hat{\boldsymbol{u}} = \hat{\boldsymbol{d}}_s - \boldsymbol{r}$ is the unit vector from the surface to the Sun, $\hat{\boldsymbol{d}}_s$ is the position vector of the Sun relative to the Earth, B is a scattering coefficient that describes the fraction of light scattered normal to the surface (equal to 2/3 for an ideal Lambertian surface), and $H(\boldsymbol{u})$ is the visibility function for the surface and is equal to 1 when the Sun is in view and 0 otherwise.

As there is no method to incorporate this physically realistic SRP model with a lack of a priori information (i.e., object geometry, attitude behavior, surface properties, thermal characteristics, etc.), and because a systematic study of the entire parameter space represents a difficult and laborious task,[2] several simplifications must be made. We have shown in Rosengren and Scheeres (2014) that if the net direction in which the SRP acceleration acts lies within the Earth's heliocentric orbit plane, the object will have similar dynamics to a cannonball. Therefore, the main non-cannonball effects are associated with the out-of-plane component of solar radiation pressure. For simplicity, consider a flat plate object which maintains a fixed orientation with respect to the Earth-Sun line. The disturbing acceleration—in the case of perfect specular reflection ($\rho s = 1$)—can be represented as

$$\boldsymbol{a}_{srp} = -\frac{2(A/m)P_\Phi\left(\hat{\boldsymbol{n}} \cdot \hat{\boldsymbol{d}}_s\right)^2}{d_s^2}\hat{\boldsymbol{n}} \tag{17}$$

where we assume that the object is close to the Earth, or $r \ll d_s$, and we ignore the possible effect of the object passing through the Earth's shadow. The surface normal direction can be specified as

$$\hat{\mathbf{n}} = \cos\theta\cos\phi\hat{\boldsymbol{d}}_s - \cos\theta\sin\phi\hat{\boldsymbol{d}}_{s_\perp} + \sin\theta\hat{\boldsymbol{H}}_s \tag{18}$$

where $\hat{\boldsymbol{d}}_{s_\perp} = \widetilde{\hat{\boldsymbol{H}}}_s \cdot \hat{\boldsymbol{d}}_s$.

Simulations have been carried out for a range of HAMR objects, released from the Laplace plane graveyard orbit with effective area-to-mass ratios from 0 up to 40 m^2/kg. The SRP acceleration, Eq. (17), was averaged over the object's unperturbed orbit and included in the averaged model developed in Rosengren and Scheeres (2013). The angle θ in Eq. (18) was varied between 0° and 90° and ϕ assumed a value between −45° and 45°. For the object with $\phi = 0°$, the evolution in the (i, Ω) phase space is similar to what was predicted using the cannonball model (Rosengren and Scheeres, 2014). When the SRP acceleration direction is tilted out of the ecliptic plane, the symmetry of the motion about the modified Laplace plane is eradicated for large values of ϕ. Nevertheless, in all cases considered, these HAMR objects if started from this inclined graveyard orbit never crossed through zero inclination over a hundred year evolution. Moreover, only the objects that are in near resonance with the Saros (17 m^2/kg $\leqslant (1+\rho)A/m \leqslant 25$ m^2/kg) (q.v., Rosengren and Scheeres, 2013) came within 5° of the geostationary orbit.

4. Economic viability and alternative disposal option

The current disposal orbits (Fig. 4) free desirable longitudinal positions for replacement satellites and reduce immediate collision hazards in GEO with an acceptable cost-to-benefit ratio, an important criterion. The cost in

[2] McMahon and Scheeres (2010) have developed a general model for solar radiation pressure acting on natural and artificial celestial bodies that enables the forces and torques to be analyzed independent of the objects's specific characteristics. Such an analytical model is well-suited for such applications, but will not be pursued in this work.

Author's personal copy

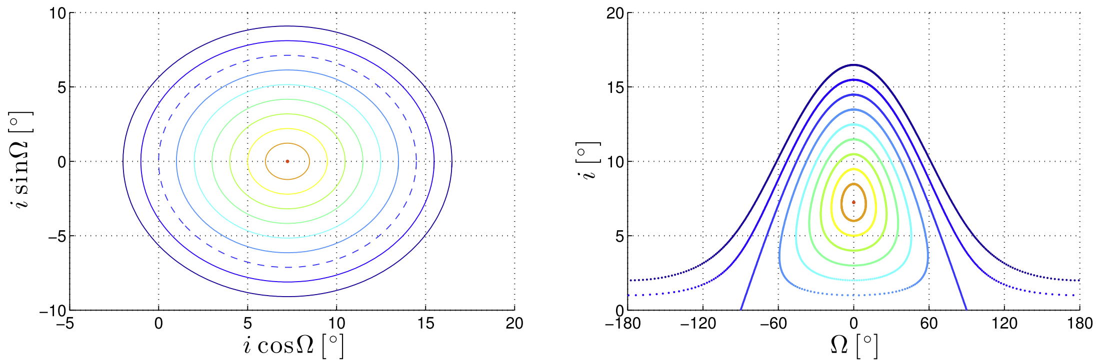

(a) Evolution as viewed from Earth's polar axis.

(b) Structure of the evolution in inclination and ascending node phase space.

Fig. 10. Qualitative evolution, over 55 years, of the orbital planes of satellites released from inclined super-synchronous orbits, showing how the alternative graveyard orbit scheme would keep objects out of the equatorial plane. The dashed curve in Fig. 10(a) and the separatrix-like curve in Fig. 10(b) are the plane precession of a satellite released from zero inclination (i.e., geostationary orbit). The classical Laplace plane equilibrium is the dot in the center of these plots.

terms of incremental velocity is not more than 3.65 m/s per 100 km increase in altitude, which amounts to the fuel needed for one month operational station–keeping (Hechler and Van der Ha, 1981). To place a satellite into the Laplace plane graveyard, not only must the current practice be implemented to remove the satellite from GEO altitude, but the satellite's orbit must be inclined by about 7.2°. This expensive plane change maneuver requires an incremental velocity of roughly 388 m/s, a third the cost of placing the satellite on an escape trajectory (for comparison, a de-orbit maneuver at GEO requires ~1.5 km/s and an Earth-escape maneuver costs ~1.2 km/s Petro (1992)). The IADC (2007) guidelines for storage orbits are based on a one-dimensional problem: define a safe minimum re-orbiting distance above GEO needed to isolate the retired satellites from GEO. It was noted, however, that these guidelines should be updated as new information becomes available regarding the space environment, as to define what constitutes an effective graveyard (IADC, 2007).

An alternative disposal option to the Laplace plane graveyard is to simply incline the current disposal orbits by a minimum inclination, as shown in Fig. 10, such that the HAMR objects released here will not cross through the geostationary orbit. For instance, a modest plane change maneuver of half a degree would only require an incremental velocity of less than 27 m/s. The basic physical principle behind this two-dimensional disposal scheme is easy to grasp. The orbit's angular momentum vector sweeps out a circular cone around the fixed pole of the classical Laplace plane, with the radius of the circular path being a function of the orbit's inclination to this fixed plane (Fig. 10a). Accordingly, tilting the orbit normal towards the axis of the Laplace plane shrinks this circle, and as the modified Laplace plane is further inclined, the HAMR objects released here will not cross below the initial inclination of the disposal orbit.

5. Conclusion

The importance of managing space debris is acknowledged by all space-faring nations, as the long-term financial, legal, and environmental implications of collisions between high-value satellites are manifest. The discovery of the high area-to-mass ratio debris reveals that the situation in the geostationary orbit region is even more critical than previously thought, and is becoming as compelling a problem as in LEO. As we begin to discover the full scope of the debris problem in GEO, we are finding that the current graveyard and mitigation practices are now obsolescent. We have used our understanding of the classical and modified Laplace planes for the identification of robust GEO disposal orbits. In accordance with Friesen et al. (1993), we propose the use of the stable Laplace plane equilibrium as a long-term graveyard for GEO. Based on our analysis of the modified Laplace plane, we showed that if satellites located in the classical Laplace plane graveyard orbit shed HAMR objects, their orbits will be trapped in (i, Ω) phase space, and will not likely cross through geostationary orbit. This new graveyard region, being surrounded by closed precessional trajectories (Fig. 10b), may also be robust for the containment of objects released from an explosion or fragmentation event; although future numerical studies are needed to confirm this proposition. The Laplace plane graveyard orbit is, in some sense, analogous to the ocean gyres which are characterized by exceptionally high concentrations of marine debris that have been trapped by the currents (Law et al., 2010). This analogy is, however, misleading as to the nature of these stable environments: the currents naturally bring floating debris toward the ocean gyres, whereas it is up to the spacecraft operators to place their retired satellites in the Laplace plane. For this reason, we proposed an alternative, cost-effective graveyard orbit based on the structure of the orbit plane evolution in the

Author's personal copy

(i, Ω) phase space. Future trade space studies are needed to determine the minimum inclination that will yield the optimum cost-to-benefit ratio, and innovative methods that take advantage of the natural forces to effect the plane change are desired.

Acknowledgements

This material is based upon work supported by the National Science Foundation Graduate Research Fellowship under Grant No. DGE 1144083. D.J.S. acknowledges support from Grant FA9550-11-1-0188, administered by the Air Force Office of Scientific Research.

References

Allan, R.R., Cook, G.E., 1964. The long-period motion of the plane of a distant circular orbit. Proc. R. Soc. Lond. A 280, 97–109.
Allan, R.R., Cook, G.E., 1967. Discussion of paper by S.J. Peale, 'Dust Belt of the Earth'. J. Geophys. Res. 72, 1124–1127.
Anselmo, L., Pardini, C., 2010. Long-term dynamical evolution of high area-to-mass ratio debris released into high Earth orbits. Acta Astronaut. 67, 204–216.
Boué, G., Laskar, J., 2006. Precession of a planet with a satellite. Icarus 185, 312–330.
Friesen, L.J., Jackson, A.A., Zook, H.A., Kessler, D.J., 1992. Analysis of orbital perturbations acting on objects in orbits near geosynchronous Earth orbit. J. Geophys. Res. 97, 3845–3863.
Friesen, L.J., Kessler, D.J., Zook, H.A., 1993. Reduced debris hazard resulting from a stable inclined geosynchronous orbit. Adv. Space Res. 13, 231–241.
Früh, C., Schildknecht, T., 2012. Variation of the area-to-mass ratio of high area-to-mass ratio space debris objects. Mon. Not. R. Astron. Soc. 419, 3521–3528.
Graf Jr., O.F., 1975. Lunar and solar perturbations on the orbit of a geosynchronous satellite. In: Proceedings of the AAS/AIAA Astrodynamics Specialist Conference, Nassau, Bahamas, Paper AAS 75-023.
Hechler, M., Van der Ha, J.C., 1981. Probability of collisions in the geostationary ring. J. Spacecr. Rockets 18, 361–366.
Inter-Agency Space Debris Coordination Committee. IACD Space Debris Mitigation Guidelines. IACD-02-01, 2002; revised 2007.
International Telecommunication Union, 2010. Environmental protection of the geostationary-satellite orbit. ITU-R S. 1003-2.
Johnson, N.L., 1982. The development and deployment of Soviet geosynchronous satellites. J. Br. Interplanet. Soc. 35, 450–458.
Johnson, N.L., 2012. A new look at the GEO and near-GEO regimes: operations, disposals, and debris. Acta Astronaut. 80, 82–88.
Kessler, D.J., Cour-Palais, B.G., 1978. Collision frequency of artificial satellites: the creation of a debris belt. J. Geophys. Res. 83, 2637–2646.
Kudielka, V., 1994. Balanced Earth satellite orbits. Celestial Mech. Dyn. Astron. 60, 455–470.
Law, K.L., Morét-Ferguson, S., Maximenko, N.A., et al., 2010. Plastic accumulation in the North Atlantic subtropical gyre. Science 329, 1185–1188.
Liou, J.-C., Johnson, N.L., 2006. Risks in space from orbiting debris. Science 311, 340–341.
Liou, J.-C., Weaver, J.K., 2005. Orbital dynamics of high area-to-mass ratio debris and their distribution in the geosynchronous region. In: Proceedings of the Fourth European Conference on Space Debris, Darmstadt, Germany, Paper ESA SP-587.
McMahon, J., Scheeres, D., 2010. Secular orbit variation due to solar radiation effects: a detailed model for BYORP. Celestial Mech. Dyn. Astron. 106, 261–300.
McMahon, J.W., Scheeres, D.J., 2013. High-fidelity solar radiation pressure effects for high area-to-mass ratio debris with changing shapes. In: Proceedings of the AAS/AIAA Astrodynamics Specialist Conference, Hilton Head, South Carolina, Paper AAS 13-763.
Mignard, F., Hénon, M., 1984. About an unsuspected integrable problem. Celestial Mech. Dyn. Astron. 33, 239–250.
Milankovitch, M., 1941. Kanon der Erdbestrahlung und seine Anwendung auf das Eiszeitenproblem, Königlich Serbische Akademie, (in German). (Canon of Insolation and the Ice-age Problem, Israel Program for Scientific Translations, 1969).
NASA Orbital Debris Program Office, 2012. Two derelict NOAA satellites experience anomalous events. In: Liou, J.-C., Shoots, D. (Eds.) Orbital Debris Quarterly News, vol. 16, (1).
Petro, A.J., 1992. Techniques for orbital debris control. J. Spacecr. Rockets 29, 260–263.
Richter, K., Keller, H.U., 1995. On the stability of dust particle orbits around cometary nuclei. Icarus 114, 355–371.
Rosengren, A.J., Scheeres, D.J., 2013. Long-term dynamics of high area-to-mass ratio objects in high-Earth orbit. Adv. Space Res. 52, 1545–1560.
Rosengren, A.J., Scheeres, D.J., 2014. On the Milankovitch orbital elements for perturbed Keplerian motion. Celestial Mech. Dyn. Astron.. http://dx.doi.org/10.1007/s10569-013-9530-7.
Rosengren, A.J., Scheeres, D.J., McMahon, J.W., 2013a. Long-term dynamics and stability of GEO orbits: the primacy of the Laplace plane. In: Proceedings of the AAS/AIAA Astrodynamics Specialist Conference, Hilton Head, South Carolina, Paper AAS 13-865.
Rosengren, A.J., Scheeres, D.J., McMahon, J.W., 2013b. The classical Laplace plane and its use as a stable disposal orbit for GEO. In: Proceedings of the Advanced Maui Optical and Space Surveillance Technologies Conference, Maui, Hawaii.
Scheeres, D.J., 2012. Orbit mechanics about asteroids and comets. AIAA J. Guid. Cont. Dyn. 35, 987–997.
Schildknecht, T., 2007. Optical surveys for space debris. Astron. Astrophys. Rev. 14, 41–111.
Schildknecht, T., Musci, R., Ploner, M., et al., 2004. Optical observations of space debris in GEO and in highly-eccentric orbits. Adv. Space Res. 34, 901–911.
Tremaine, S., Touma, J., Namouni, F., 2009. Satellite dynamics on the Laplace surface. Astron. J. 137, 3706–3717.
Ulivieri, C., Circi, C., Ortore, E., et al., 2013. Frozen orbital plane solutions for satellites in nearly circular orbit. J. Guid. Cont. Dyn. 36, 935–945.
Zee, C.-H., 1989. Theory of Geostationary Orbits. Kluwer Academic Publishers.